Surface & Coatings Technology 457 (2023) 129268

Contents lists available at ScienceDirect

Surface & Coatings Technology

journal homepage: www.elsevier.com/locate/surfcoat

A two-stage approach to Ni-P-SiC coatings and their friction against SiC in water

Zhechen Zhang [a], Chenbo Ma [b], Qinqwen Dai [a], Wei Huang [a,*], Xiaolei Wang [a]

[a] College of Mechanical & Electrical Engineering, Nanjing University of Aeronautics & Astronautics, Nanjing 210016, China
[b] College of Mechanical & Electrical Engineering, Nanjing Forestry University, Nanjing 210037, China

ARTICLE INFO

Keywords:
Ni-P-SiC coating
Low friction
Water lubrication
Tribochemical wear

ABSTRACT

Inspired by the low friction of self-mated SiC in water, a two-stage technique is proposed to deposit Ni-P-SiC coating with a high particle content to achieve low friction against SiC in water. The process comprises the electrophoretic deposition of SiC particles layer on a mild steel substrate followed by the electroless plating of Ni—P coating. The effects of SiC content on the surface appearance, phase structure and cohesive strength were studied. Much attention was paid on the friction behavior of the coatings in water. Experiment results show that compared with the traditional electroless plating method, the two-stage technique can enhance the implanted SiC particle content effectively. Notable, with the increasing of SiC content, the friction coefficient decreases correspondingly and the lowest friction coefficient of 0.015 can be achieved for the Ni-P-SiC coatings with the highest SiC particle content. The major surface degradation mode is abrasive wear during running-in then tribochemical wear dominates at the low friction stage.

1. Introduction

Oil lubricants play an important role in the modern industry. Nowadays, with the energy shortage and environment deterioration, there is an urgent need for alternatives. Recently, water lubrication is getting great interest due to its merits of friendly environment, flame retardant and low cost. While for water lubrication, one of the main pain points is to seek the proper materials as the moving elements [1].

Ceramics, such as SiC and Si_3N_4, are good candidates as water lubricated materials. The low friction coefficients of 0.01–0.001 can be obtained for self-mated SiC and Si_3N_4 tribopairs during sliding in water with negligible wear [2–6]. Proposed suggestions are attributed to hydrodynamic lubrication after ultra-smooth contact surface is formed by tribochemical wear [5,7]. Although the Si-based ceramics present excellent water lubrication behavior, the issues of hard machinability, low fracture toughness and high processing cost remain fairly serious [8].

Composite electrodeposition is a conventional technology to fabricate composite coatings [9]. In this area, much outstanding research has been done by F.C. Walsh et al. [10–15]. Besides electrodeposition, electroless composite deposition is also a handy coating preparation technique [16], which uses the conventional reduction reaction process with suspensions of particles. During the course of reduction, metallic composite coating can be obtained from a solution containing suspended fine particles. Various second phases in electroless metallic coatings may achieve desirable properties. The hardness of the coating increases with the increased amount of hard particles (SiC) [17], and the value also decreases with the soft particle (PTFE) [18]. In addition, the wear (SiC and Al_2O_3) [19,20] and corrosion (CeO_2) [21] resistance and self-lubrication(PTFE) [22] can also be improved by the incorporation of second phase.

As mentioned above, advanced engineering ceramics offer unique capabilities as tribomaterials in water. Compared with other ceramics (Si_3N_4, Al_2O_3 and ZrO_2), SiC material can achieve low friction coefficient at the higher mean contact pressure [23]. Up to now, only self-mated SiC is applied successfully in mechanical water seals or water lubricated bearings [24]. In view of the outstanding friction performance of bulk SiC in water, how about the water lubrication properties of the composite coating embedded with tiny SiC particles? If the idea works, the most promising tribological application areas of the coatings could be sliding components, such as ceramic sliding bearings. Actually, the mechanical and tribological performances of electroless plating Ni-P-SiC coating have been reported widely [25–29]. However, few details could be gleaned about the its frictional behavior in water. Besides,

* Corresponding author at: Yudao Street 29#, Nanjing, China.
E-mail address: huangwei@nuaa.edu.cn (W. Huang).

https://doi.org/10.1016/j.surfcoat.2023.129268
Received 3 December 2022; Received in revised form 16 January 2023; Accepted 17 January 2023
Available online 25 January 2023

for the traditional electroless plating method, the content of SiC particle incorporated to Ni-P-SiC coating is relatively low, usually below 10 wt% [25–27]. While the properties of the coating depend heavily on the content of the second phase particles. Is there any other way to further improve the content of the SiC in the coating so as to achieve a better water lubrication behavior? There is still no available knowledge about this.

In this paper, preliminary studies of a two-stage technique are proposed to fabricate the Ni-P-SiC composite coating. Fig. 1 shows the main preparation process. Firstly, a layer of SiC particles is deposited on a substrate by an electrophoretic deposition method. In the second stage, taken accounting of the safety and economy, electroless planting Ni—P is performed to cover the partial layer of the particles. In this process, the electrolyte passes through the gaps between SiC particles to the substrate and reduction of nickel from ion follows immediately. The final composite coating can be obtained after wiping off the unburied particles. The effects of SiC content on the surface appearance, phase structure and cohesive strength were studied. Much attention was paid on the friction behavior of the Ni-P-SiC coating in water.

2. Experimental details

2.1. Electrophoretic deposition of SiC layer (first stage)

The coating was fabricated on a substrate of flat 45 steel with the size of Φ30 × 3 mm. The surface of the steel was ground and mechanically polished to the roughness *Ra* of 100 ± 10 nm. Then it was degreased ultrasonically in acetone for 10 min, activated with a 10 vol% solution of HCl for 1 min and rinsed in deionized water. Subsequently, the electrophoresis was carried out in an ethanol bath (beaker 500 mL) including commercially available SiC particles (6 and 8 g/L). The sizes of the particle are mainly in the range of 600–800 nm with an irregular shape. In addition, $MgCl_2{\cdot}6H_2O$ with the concentration of 0.2 g/L was also dissolved in the ethanol bath as dielectric medium. In the case of standing, particle sedimentation occurs obviously. To avoid particle sedimentation and ensure the particle suspending homogenously, the solution was agitated during the deposition with a magnetic stirring at a rate of 300 rpm. According to the Reynolds number, the flow regime of the solution could be turbulent. The olive-shaped magnetic stirrer was completely PTFE-coated. And its position is at the center of the beaker bottom. Vertically and parallelly placed electrodes were immersed in the ethanol with a distance of 3.5 mm. Two voltages of 35 and 50 V were applied between the electrodes with the corresponding electric field intensity of 10.0 and 14.3 V/cm, respectively. The electrical conductivity of the electrophoretic bath is about 40 μS/cm. Since the particles are preferential absorbing of positive ion in the electrophoretic solution, the deposition happens on the cathode. The time of each electrophoresis was fixed at 2 min.

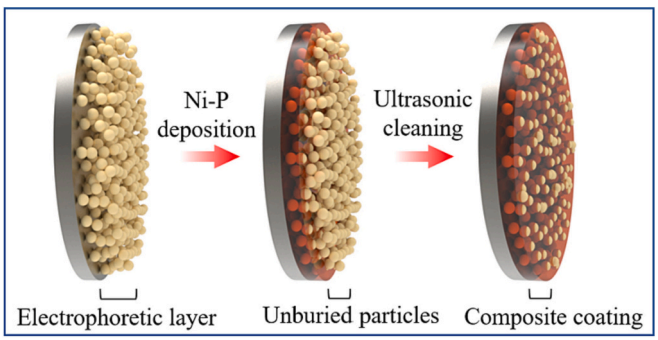

Fig. 1. Schematic diagram of the two-stage technique.

2.2. Electroless plating of Ni—P coating (second stage)

In the second stage, the specimen deposited with a SiC film was transferred into deionized water to dilute redundant ethanol. Then, it was subjected to electroless plating of Ni—P in a beaker (500 mL). Table 1 shows the composition of the plating bath, without any SiC particles. The nickel ion source was nickel sulphate and sodium hypophosphite played as the nickel ion reducing substance. Sodium acetate was responsible for buffering the bath. To protect the electrophoretic layer from falling off due to the brisk evolution of hydrogen gas, the low bath temperature of 65 °C with the pH value of about 6.0 was applied. Each plating time was set at 90 min. During this process, nickel ion may preferentially pass through the pores of the loose SiC film and the tiny inter-particle spacing will be filled with the reduced Ni—P. Thus, the ceramic particles can be held and bonded tightly within the metallic matrix. At last, the coatings were cleaned in running water, followed by ultrasonic cleaning in acetone to eliminate the extra unburied SiC particles.

For comparing, Ni—P and Ni-P-SiC coatings were also fabricated by the traditional electroless plating (one-stage method) [18]. The suspending particle concentrations of the plating bath were controlled at 0 and 10 g/L, respectively. The bath was stirred by a magnet stirring with a rate of 300 rpm. To increase the deposition rate, the bath temperature increased to 80 °C, which is different from the two-stage method. Other details of bath composition and operating parameters can be found in Table 1.

2.3. Characterization methods

The surface and cross sectional appearances of the coatings were observed by a scanning electron microscope (SEM) equipped with an energy dispersive spectrometer (EDS) (Quanta 200, Philips-FEI, Netherlands). The phase structure of the prepared samples was characterized by an X-ray diffraction (X'Pert PRO, Panalytical, Netherlands). To estimate the cohesive strength of the coatings, scratch test was performed with a progressive loading speed of 10 N/mm.

The water lubrication experiment of the coatings was carried out by using a ball-on-disk tribometer. To compared with the self-mated bulk SiC, a SiC ball (Φ 8 mm) was chosen as the counterpart. The coating sample fixed with a rotating cup and The contact surface was fully submerged in deionized water. The sliding speed of 0.25 m/s was set with a normal load of 2 N. The friction coefficient was recorded during the sliding time of 20 h. The worn surface was evaluated by SEM and the volumetric material loss was measured by a 3D profilometry. Wear rate (cm^3/N m) of the tribopairs was estimated by dividing the loss of wear volume by the normal load and sliding distance. To further explore the wear mechanism, a micro conductivity meter was used to monitor a real-time change of the lubricant electrical conductivity accompanying by the sliding process. Besides, a transmission electron microscope (TEM, JEM-200CX, JAP) was applied to observe the wear products dispersed in the water.

Table 1
Composition of the bath and the plating parameters.

Constituent	Component	Amount (g/L)
Main salt	Nickel sulfate ($NiSO_4 \bullet 6H_2O$)	30
Reducing agent	Sodium hypophosphite ($NaH_2PO_2 \bullet H_2O$)	26
Complexing agent	Lactic acid ($C_3H_6O_3$)	18
	Propanoic acid ($C_3H_6O_2$)	4
Buffering agent	Sodium acetate ($C_2H_3NaO_2 \bullet 3H_2O$)	15
Stabilizing agent	Thiourea (CH_4N_2S)	0.002
pH		6.0
Temperature (°C)		65
Loading ratio (dm^2/L)		0.28
Plating time (min)		90

3. Results and discussion

3.1. Morphologies, compositions and phase structures

The surface and cross section appearances of the five coatings are shown in Fig. 2. Obvious differences are observed between the surface of the Ni—P and Ni-P-SiC coatings. The Ni—P coating presents a very flat and continuous surface with some tiny nodular structures. The coating surface containing the second phase particles looks completely different. It has a gray rough surface dispersed with many micro-bulges ranged from 5 to 10 μm in size. Even so, the composite coatings are still dense without significant difference. Elements Si and C are detected on the surfaces, which confirms the existence of SiC in the coatings. According to the data of the EDS, it can be found that the SiC content in the coating fabricated by traditional electroless plating (one-stage method) is about 7.25 wt%. While for the two-stage method, the particle content of Ni-P-SiC coating (35 V, 6 g/L) improve to 11.50 wt% and the value reaches 14.35 wt% as the bath concentration of SiC increases to 8 g/L. Increasing the electrophoresis voltage may cause a further enhancement of particle content in the composite coating (50 V, 8 g/L) to 17.59 wt%. Actually, during the electrophoretic deposition, the particle packing density of the SiC layer has been calculated based on mass per unit area. For sample (35 V, 6 g/L), the packing density of the SiC layer is 2.8 mg/cm^2. And the values increased to 4.9 mg/cm^2 for sample (35 V, 8 g/L) and 7.3 mg/cm^2 for sample (50 V, 8 g/L). According to the Hamaker's equation [30], mass of the deposit has a linear relationship with the particle concentration in suspension and the strength of electric field. The incorporation percentage of SiC particles in the deposits increases with the increasing electrophoresis voltage and the particle concentration of the electrophoretic solution.

The increment of the embedded SiC content may also be conformed from the cross sectional analysis. As can be seen, the inner part of the coatings is compact, without any cracks or pores. Comparing to the pure Ni—P coating, uniformly dispersed SiC particles are enveloped by metallic matrix. The Si content in the cross section presents almost the same variation trend as that of the surface and the coatings obtained from the two-stage method present the higher content in general. Similarly, the higher particle concentration and voltage, the higher particle content. Such result indicates again the two-stage method may obtain the Ni-P-SiC composite coating with high particle content.

The XRD patterns of the Ni—P and Ni-P-SiC composite coatings are given in Fig. 3. It can be seen that the Ni—P coating contains only one peak of Ni (JCPDS Card. No.70-0989). In addition, all the peaks of Ni are broad, which reveal that in the as-deposited state, the samples are amorphous either with or without SiC. The overlapped sharp peaks at approximately $2\theta = 45^\circ$ were from the 45 steel substrate [18]. For the two Ni-P-SiC samples (35 V, 6 g/L and 35 V, 8 g/L), the implanted SiC particles do not show any visible effect on the coatings' structure. With the increase of the particle content, for the Ni-P-SiC sample (50 V, 8 g/L), additional reflection plane of (111) can be observed for cubic β-SiC

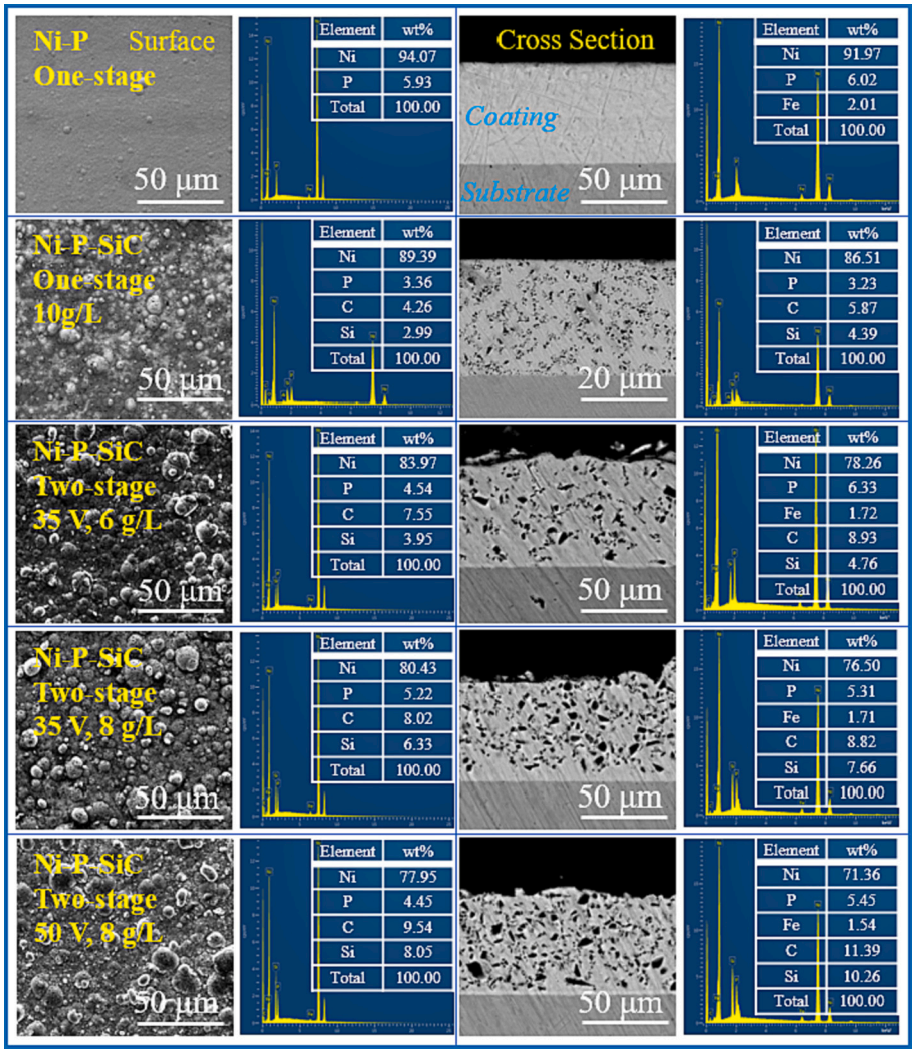

Fig. 2. SEM, EDS and cross section images of the Ni—P and Ni-P-SiC composite coatings.

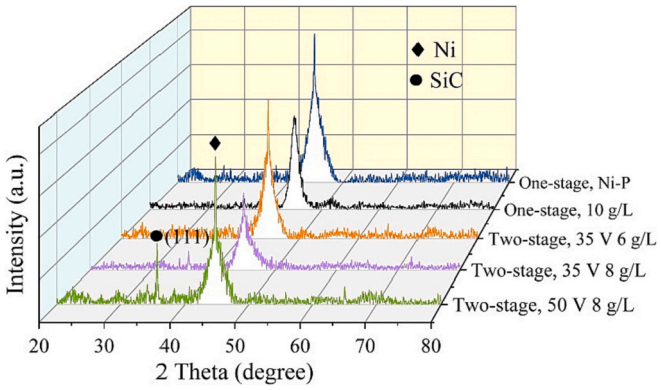

Fig. 3. XRD patterns of the Ni—P and Ni-P-SiC composite coatings.

phase at Bragg's angles 36° (JCPDS Card. No.29–1129). Hence, the XRD pattern demonstrates the existence of SiC in the composite coating, which is in agreement with the SEM results.

3.2. Scratch resistance

The scratch test is an effective approach to elevate the cohesive strength of coating. During the scratching process, an indenter of a well-defined tip is drawn across the surface of a coating under an increasing load. The load, corresponding to the first crack appearance is defined as the cohesive load and it represents the intrinsic strength of the film [31]. Fig. 4 presents the optical micrographs of the scratched surfaces on the coatings and the scratch width increases gradually with the increasing load. Due to the nature of ductile, Ni—P coating possesses the highest cohesive strength and no crack is observed when the load increases to 30 N. For the composite coatings, the cohesive strength decreases obviously and the cohesive load seems to be related to the SiC particles content.

When an indenter scratching the coating with an increasing load, deformation of the coating occurs, and this deformation is purely elastic at the beginning of the test. As the load increases, a critical point is reached at which the elastic limit of the coating is exceeded and plastic deformation starts. Once full plasticity is reached, the plastic flow should occur in the coating surface. The horizontal force acting on the coating should be made up of three components. The first one is the ploughing force required to deform the coating. The second is the force needed to shear the cohesive bond of coating. The third component is the force required to push aside the sheared film [32].

The reduced cohesive strength could be taken into consideration from two aspects: the internal stress and dislocation. As pointed in Ref. [33], the cohesive strength of the coating relies heavily on the internal stress. When SiC particles are implanted into metallic matrix, because of the different coherency strains in the interface/matrix, the defects or lattice deformations appear, which may significantly increase the internal stress and reduce the cohesive strength of the composite coating. Besides, the movement of dislocations could be the other reason [16]. Due to embedded particles, the propagate of the dislocation may take a path around the particles. With the increment of the particle content, it will be more convenient for the dislocation to loop between particles rather than to cut through them. Thus, the higher content of the particles, the lower cohesive strength.

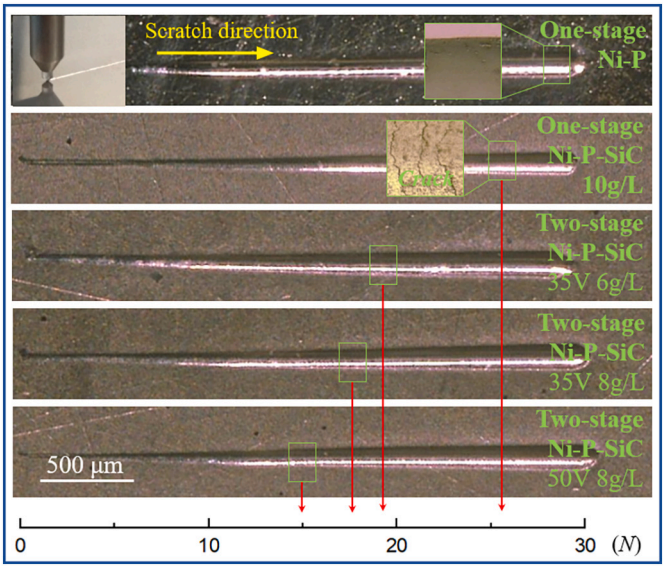

Fig. 4. Optical images of the scratch on the Ni—P and Ni-P-SiC composite coatings.

3.3. Water lubrication properties

Fig. 5 shows the variations of the friction coefficient of the Ni—P and Ni-P-SiC composite coatings in water. After sliding in water for 20 h, the Ni—P coating always possesses the largest average friction coefficient of about 0.18 and it fluctuates between 0.15 and 0.22. The coefficients decrease significantly for the Ni-P-SiC composite coatings. For the one-stage method prepared sample, the value declines continuously and the it reaches to 0.075 at the end of the 20 h test. The coefficients of the three two-stage technique prepared Ni-P-SiC coatings are lower than that of the one-stage prepared sample in general. Their coefficients decrease obviously at the first 3 h and the values remain stable for the two samples (35 V, 6 and 8 g/L) with the lower SiC content. With the increase of the sliding time, the friction coefficients of the two samples reduce again and the final values stabilize at 0.025. While for the sample with the highest SiC particle content (50 V, 8 g/L), the coefficient continues to fall after sliding for 14 h and the lowest value of 0.015 can be achieved. According to the variations of the frictional curves, it is believed that implanted particle concentration in the Ni—P matrix plays crucial influence on the coatings' water lubrication property.

Fig. 6 shows the wear rates of the five samples and corresponding balls after sliding in water for 20 h. As can be seen, the Ni—P coating presents the highest wear rate. Wear rates decrease with the increment of the SiC content and the sample with the highest SiC particle content (50 V, 8 g/L) shows the lowest wear rate. During the sliding process, the reinforced particles may avoid the direct contact between the upper ball

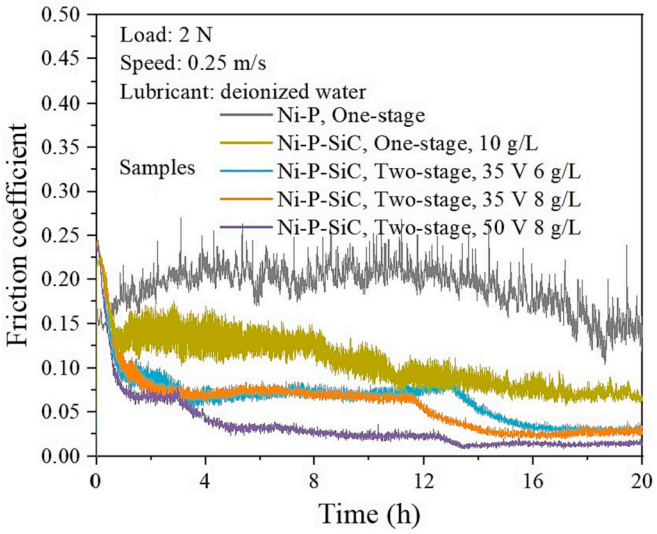

Fig. 5. Variations of the coefficients of friction for the five coatings.

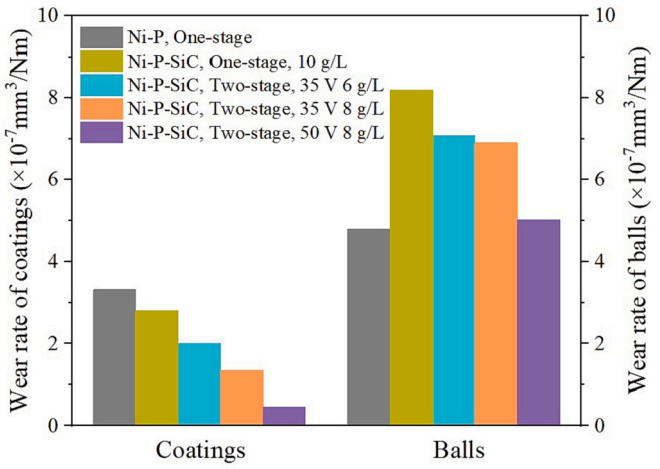

Fig. 6. Wear rates of the coatings and corresponding balls.

and matrix to a certain extent and the adhesion wear is slowed down. Besides, as pointed in Ref. [34], the dispersion hardening effect, which results from the implanted SiC particles, is the other reason for the enhanced wear resistance.

While for the balls, different results occur and the ball sliding on the Ni—P coating expresses the lowest material removal rate. With the increment of SiC content in the matrix, the wear rate improves obviously. Such result indicates that the embedded ceramic particles may not only work as the bearing unit to enhance wear resistance of the coating, but play as micro-cutting tool to improve the material removal rate of the ball. However, the value of the ball decreases while sliding against the coating with the highest particle content (50 V, 8 g/L). The reason could be related with the corresponding wear mechanism of tribochemical reaction [6], which will be discussed in the subsequent section.

To further understand the reason of the low friction, variations of the conductivity of the lubricant, the worn surfaces as well as the contact pressure for the two-stage prepared sample (50 V, 8 g/L) were investigated at several typical friction moments. As shown in Fig. 7, the initial friction coefficient is about 0.25 and it decreases dramatically. Accompanying by the sliding, the electrical conductivity of the water grows steadily. According to the calculation of Gibb's free energy, the following tribochemical reaction between the SiC and water (Eq.1) are suggested [7]:

$$SiC + 2H_2O \rightarrow SiO_2 + CH_4;\ \Delta G = -369.1\ kJ/mol \quad (1)$$

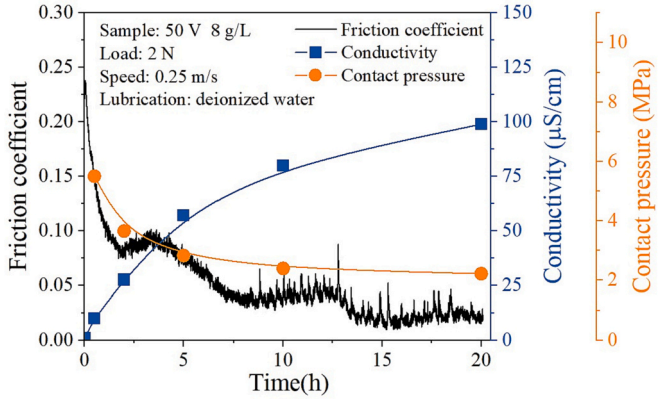

Fig. 7. Variations of contact pressure and lubricant conductivity at different friction stages (Ni-P-SiC composite coating fabricated by two-stage method, 50 V, 8 g/L).

$$SiO_2 + 2H_2O \rightarrow Si(OH)_4;\ \text{hydration} \quad (2)$$

And then, the hydrolysis reaction of the SiO_2 occurs (Eq. (2)), which is mechanically induced at the sliding interface by friction [35]. It has been postulated that a tribolayer of silica gel or silicic acid can be formed between the self-mate SiC. Thus, the in-situ formation of this tribolayer might lower the stress of shearing at the contact interface. Recent works also show that the existence SiO_2 layer in the interface may not only reduce friction but improve hydrophilicity [36]. According to Xu and Kato [4], the electrical conductivity may indirectly reflect the changes of ions concentration during sliding and the kinetics of tribochemical reactions. The sustainable growth of the conductivity implies that the ions concentration increases with the sliding process. Therefore, it is believed that the low friction may be ascribed to the lubrication effect of the tribochemical reactions.

Fig. 8 shows the variations of wear surfaces at different friction moments. The flat and smooth surface has been formed on the SiC ball after sliding in water for 0.5 h. However, the wear track on the coating surface is discontinuous, exhibiting abrasion induced grooves. At this stage, contact mainly happens between the micro-bulges and the ball, which is intermittent. And the abrasive wear should be the dominant mechanism. As the sliding continues, the wear scar on the ball presents no obvious change except the scar diameter. But the track on the coating becomes deeper and wider, which may help to decrease the contact pressure. More importantly, the roughness of the track drops significantly according the 3D and the cross profile images.

Fig. 9 shows the comparison of the original and the final SEM images of the wear surface. It can be seen more clearly that lots of micro-bulges dispersed on the initial surface are grinded and the uneven surface becomes much flat and smooth. In addition, the implanted SiC particles are also worn smooth. The main elements of Ni, P, Si and C are detected. According to Ref. [4,24], as the friction coefficient decreases, the wear mechanism changes from the previous mechanical to tribochemical wear. It can be concluded that the tribochemically smoothened surface has a fundamental role to achieve the stable low friction coefficient of 0.015.

Due to the friction, the contact pattern may also change from the point to flat-on-flat geometry. And the apparent contact pressure varies as well (see in Fig. 7) At the beginning of the test, the pressure is high due to the corresponding contract pattern. Shortly afterwards, based on the diameter of the wear scar on SiC ball, the apparent mean contact pressure can be calculated. As shown in Fig. 7, the pressure drops quickly at the first 5 h and the value tends to be gentle till the end of the test (2.3 MPa). Similar result was reported by Chen et al. [24] and they observed the pressure for self-mated SiC entering into the low friction regime was about 4 MPa. Accompanied by friction, the apparent contact area enlarges and the mean contact pressure decreases consequentially. Actually, there is no necessary association between the lowering of friction and the reduced contact pressure. However, when considering the load carrying capacity of the lubrication film, the lubrication mechanism may change with the mean contact pressure [23], which can affect the friction coefficient indirectly. And the lubrication mechanism mainly depends on two aspects. One is the contact surface and the other is the lubrication film. Along with the sliding, contact surfaces become more smooth due to the tribochemical reaction. Thus, the mean asperities contacts decrease obviously and the friction interface possesses better conforming by wear [7]. Besides, tribochemical film of colloidal silica grows on wear surface, which can work as effective lubricant [6]. Therefore, the lubrication mechanism may change from the mixed to hydrodynamic lubrication.

At the very beginning, the contact pressure is relatively high. The low viscosity of water alone is difficult to produce enough hydrodynamic lift to provide low friction. As sliding goes on, flat-on-flat contact forms. As shown in Fig. 8, since the surface is not smooth enough, the normal load is partly by contact of the frictional surfaces at the asperity contacts. This means the contact of the asperities may introduce stress concentration

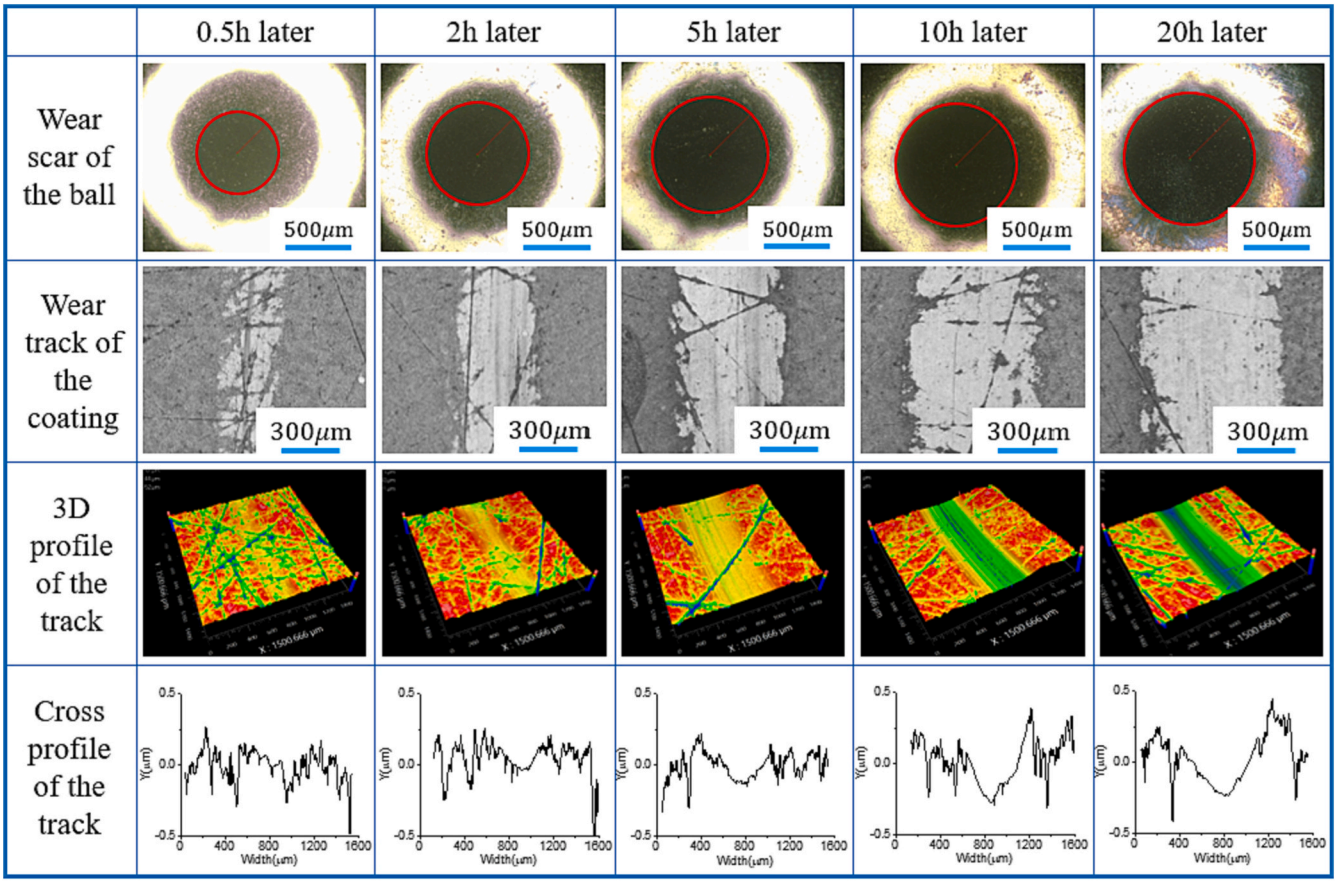

Fig. 8. Variations of wear surfaces at different friction moments (Ni-P-SiC composite coating fabricated by two-stage method, 50 V, 8 g/L).

and stress intensities excessing the load carrying capacity of the hydrodynamic film. The lubrication mechanism may be mixed lubrication, in which the states of boundary friction and fluid friction coexist. For hydrodynamics to function, the surfaces have to be smooth with a certain viscosity lubricant. Accompanied by tribochemical wear, more smoothed surface forms (see in Fig. 9), and a layer of colloidal silica with the higher viscosity generates on wear surface. Meanwhile the contact pressure also decreases to a lower value. Thus, the final low friction coefficient can be attributed to hydrodynamic lubrication after a smooth surface is obtained with a film of colloidal silica as lubricant. During the shearing process, the film is then removed from the surface by forming fine rolls or dissolved into water.

To further confirm the tribochemical reaction, the wear products suspended in the water were characterized by TEM. As shown in Fig. 10, these products present a lamellar structure with serious aggregation. The electron diffraction pattern suggests that these wear particles are polycrystalline phase. According to the EDS, elements Ni, P, O, Si and C are detected. Extremely high oxygen content may also indirectly verify the occurrence of the tribochemical reaction.

To figure out the role of the wear products, the friction test of the two-stage prepared coating (50 V, 8 g/L) were conducted again. As presented in Fig. 11, the phenomenon of low friction appears after the sample sliding in water for about 15 h. It can be deduced that the wear products and smooth surface have both been formed. After that, the water was pumped out and pure deionized water was injected. It can be noticed that the low coefficient of friction increases at once, and the value decreases gradually after sliding for another period of time. Such result further indicates that besides the smoothened surface, the wear debris generated by tribochemical reaction is the indispensable requirement to achieve the low friction.

At last, it is necessary to briefly discuss the results of scratching and friction tests. As mentioned above, the cohesive strength of the coating decreases with the increasing particle content. However, the water lubrication result shows that low friction coefficient can only be achieved for the sample with the highest SiC particle content. There is both difference and relation between the scratch and friction tests. For scratch test, the indenter is a well-defined tip. The force in the direction normal to the coating surface is increased in a controlled way. While for the friction test, a fixed normal load of 2 N is applied, which is much lower than the critical load of the scratch test. Besides, the contact patterns may change from the point momently to flat-on-flat contact. And the contact pressure also decreases to the lower values due to the enlargement of the worn surfaces. In addition, there also exists lubricants (water or colloidal silica) between the rubbing surface. Therefore, the different results between the two tests depend on specific evaluation method and application situation.

4. Conclusions

In this paper, a two-stage technique was proposed to fabricate the Ni-P-SiC composite coating. Specifically, a layer of SiC particles was electrophoretic deposited on a substrate (first stage) followed by electroless plating of Ni—P coating (second stage). The effect of SiC content on the surface appearance, phase structure and cohesive strength was studied. Much attention was paid on the friction behaviors of the coatings in water. Main conclusions are summarized as follow:

(1) The Ni-P-SiC composite coating was fabricated successfully by using the two-stage technique. Compared with traditional electroless plating, the two-stage method may improve the embedded particle content effectively. Content of the embedded SiC particles in the coating improves with the increasing electrophoresis

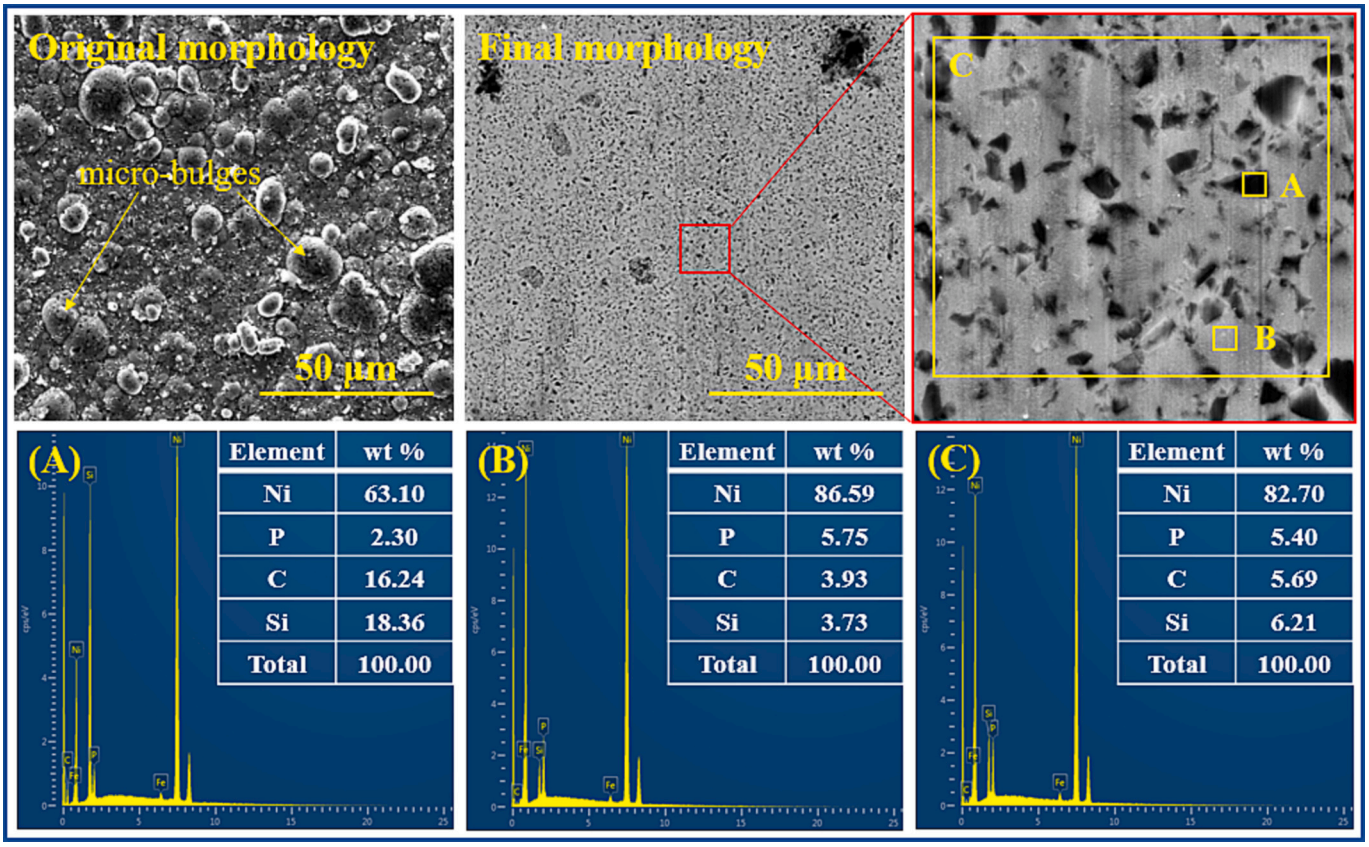

Fig. 9. Comparison of the original and the final SEM images of the wear track. The images of (A) and (B) present the EDS of small yellow square A and B; The image of (C) shows the EDS of the bigger yellow square C. (Ni-P-SiC composite coating fabricated by two-stage method, 50 V, 8 g/L). (For interpretation of the references to colour in this figure legend, the reader is referred to the web version of this article.)

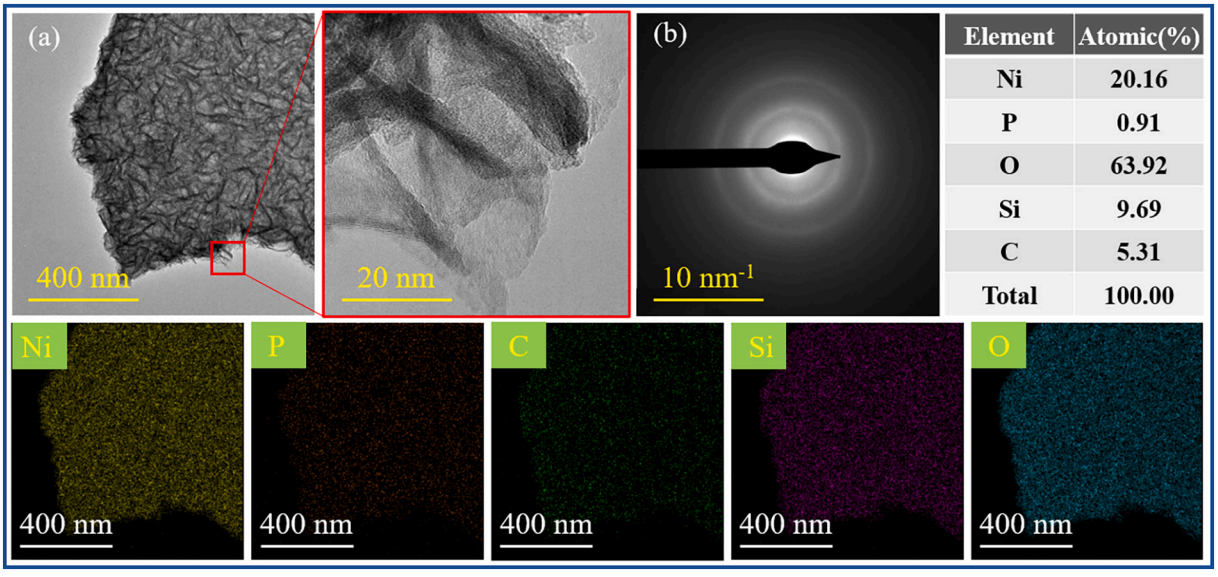

Fig. 10. TEM, electron diffraction pattern and EDS of the wear products in the water.

voltage and the particle concentration of the electrophoretic solution. The scratch test shows that cohesive strength of the coating decreases with the increasing particle content.

(2) Water lubrication results shows that low friction coefficient of 0.015 can be achieved for the sample with the highest SiC particle content. The smoothed surface and tribochemical reaction are the two requirements. Major wear mode changes from the abrasive in the stage of high friction to tribochemical wear dominated at the low friction.

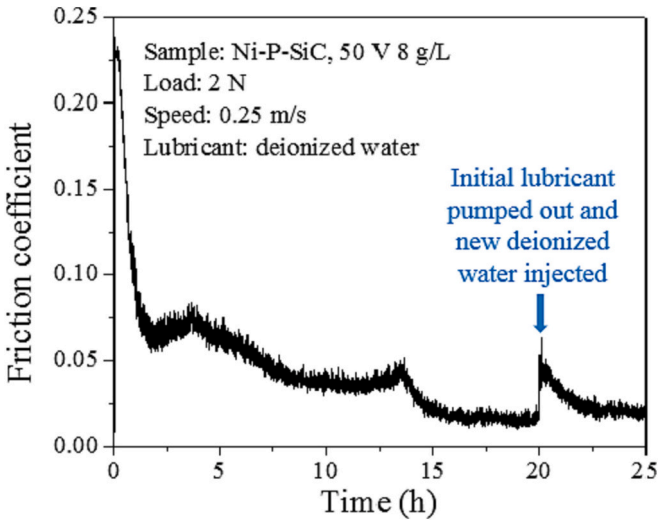

Fig. 11. Variations of the friction curve with different lubricants (Ni-P-SiC composite coating fabricated by two-stage method, 50 V, 8 g/L).

CRediT authorship contribution statement

Zhechen Zhang: Experiment and Writing-Original draft preparation.
Chenbo Ma: Data curation.
Qingwen Dai: Visualization and Investigation.
Wei Huang: Conceptualization and Writing-Reviewing and Editing.
Xiaolei Wang: Supervision.

Declaration of competing interest

The authors declare that they have no known competing financial interests or personal relationships that could have appeared to influence the work reported in this paper.

Data availability

Data will be made available on request.

Acknowledgment

The authors thank the National Key Laboratory of Science and Technology on Helicopter Transmission (Grant No. HTL-A-22G14).

References

[1] J.K. Lancaster, A review of the influence of environmental humidity and water on friction, lubrication and wear, Tribol. Int. 23 (1990) 371–389.
[2] H. Tomizawa, T.E. Fischer, Friction and wear of silicon nitride and silicon carbide in water: hydrodynamic lubrication at low sliding speed obtained by tribochemical wear, ASLE Trans. 30 (1986) 41–46.
[3] J. Xu, K. Kato, T. Hirayama, The transition of wear mode during the running-in process of silicon nitride sliding in water, Wear 205 (1997) 55–63.
[4] J. Xu, K. Kato, Formation of tribochemical layer of ceramics sliding in water and its role for low friction, Wear 245 (2000) 61–75.
[5] M. Chen, K. Kato, K. Adachi, The difference in running-in period and friction coefficient between self-mated Si3N4 and SiC under water lubrication, Tribol. Lett. 11 (2001) 23–28.
[6] R.S. Gates, S.M. Hsu, Tribochemistry between water and Si3N4 and SiC: induction time analysis, Tribol. Lett. 17 (2004) 399–407.
[7] D. Amutha Rani, Y. Yoshizawa, H. Hyuga, K. Hirao, Y. Yamauchi, Tribological behavior of ceramic materials (Si3N4, SiC and Al2O3) in aqueous medium, J. Eur. Ceram. Soc. 24 (2004) 3279–3284.
[8] L. Huang, Q. Dai, W. Huang, X. Wang, Ni/Si3N4 composite coatings and their water lubrication behaviors, Appl. Surf. Sci. 572 (2022), 151534.
[9] Y. Ootani, J. Xu, K. Adachi, M. Kubo, First-principles molecular dynamics study of silicon-based ceramics: different tribochemical reaction mechanisms during the running-in period of silicon nitride and silicon carbide, J. Phys. Chem. C 124 (2020) 20079–20089.
[10] C.T.J. Low, R.G.A. Wills, F.C. Walsh, Electrodeposition of composite coatings containing nanoparticles in a metal deposit, Surf. Coat. Technol. 201 (2006) 371–383.
[11] F.C. Walsh, C. Ponce de Leon, A review of the electrodeposition of metal matrix composite coatings by inclusion of particles in a metal layer: an established and diversifying technology, Trans. Inst. Met. Finish. 92 (2014) 83–98.
[12] F.C. Walsh, C.T.J. Low, J.O. Bello, Influence of surfactants on electrodeposition of a ni-nanoparticulate SiC composite coating, Trans. Inst. Met. Finish. 93 (2015) 147–156.
[13] K. Helle, F. Walsh, Electrodeposition of composite layers consisting of inert inclusions in a metal matrix, Trans. Inst. Met. Finish. 75 (2017) 53–58.
[14] M.S. Safavi, M. Tanhaei, M.F. Ahmadipour, R. Ghaffari Adli, S. Mahdavi, F. C. Walsh, Electrodeposited Ni-Co alloy-particle composite coatings: a comprehensive review, Surf. Coat. Technol. (2020) 382.
[15] F.C. Walsh, C. Larson, Towards improved electroplating of metal-particle composite coatings, Trans. Inst. Met. Finish. 98 (2020) 288–299.
[16] J. Novakovic, P. Vassiliou, K. Samara, T. Argyropoulos, Electroless NiP–TiO2 composite coatings: their production and properties, Surf. Coat. Technol. 201 (2006) 895–901.
[17] A. Farzaneh, M. Mohammadi, M. Ehteshamzadeh, F. Mohammadi, Electrochemical and structural properties of electroless ni-P-SiC nanocomposite coatings, Appl. Surf. Sci. 276 (2013) 697–704.
[18] Y.S. Huang, X.T. Zeng, I. Annergren, F.M. Liu, Development of electroless NiP–PTFE–SiC composite coating, Surf. Coat. Technol. 167 (2003) 207–211.
[19] I. Apachitei, F.D. Tichelaar, J. Duszczyk, L. Katgerman, The effect of heat treatment on the structure and abrasive wear resistance of autocatalytic NiP and NiP–SiC coatings, Surf. Coat. Technol. 149 (2002) 263–278.
[20] I. Apachitei, J. Duszczyk, L. Katgerman, P.J.B. Overkamp, Electroless Ni–P composite coatings: the effect of heat temperature on the microhardness of substrate and coating, Scr. Mater. 38 (1998) 1347–1353.
[21] H.M. Jin, S.H. Jiang, L.N. Zhang, Microstructure and corrosion behavior of electroless deposited Ni–P/CeO2 coating, Chin. Chem. Lett. 19 (2008) 1367–1370.
[22] A. Ramalho, J.C. Miranda, Friction and wear of electroless NiP and NiP+PTFE coatings, Wear 259 (2005) 828–834.
[23] H.-C. Wong, N. Umehara, K. Kato, Frictional characteristics of ceramics under water-lubricated conditions, Tribol. Lett. 5 (1998) 303–308.
[24] M. Chen, K. Kato, K. Adachi, Friction and wear of self-mated SiC and Si3N4 sliding in water, Wear 250 (2001) 246–255.
[25] G. Jiaqiang, L. Lei, W. Yating, S. Bin, H. Wenbin, Electroless Ni–P–SiC composite coatings with superfine particles, Surf. Coat. Technol. 200 (2006) 5836–5842.
[26] C.J. Lin, K.C. Chen, J.L. He, The cavitation erosion behavior of electroless Ni–P–SiC composite coating, Wear 261 (2006) 1390–1396.
[27] S. Zhang, K. Han, L. Cheng, The effect of SiC particles added in electroless Ni–P plating solution on the properties of composite coatings, Surf. Coat. Technol. 202 (2008) 2807–2812.
[28] C. Ma, F. Wu, Y. Ning, F. Xia, Y. Liu, Effect of heat treatment on structures and corrosion characteristics of electroless Ni–P–SiC nanocomposite coatings, Ceram. Int. 40 (2014) 9279–9284.
[29] C.-S. Chang, K.-H. Hou, M.-D. Ger, C.-K. Chung, J.-F. Lin, Effects of annealing temperature on microstructure, surface roughness, mechanical and tribological properties of Ni–P and Ni–P/SiC films, Surf. Coat. Technol. 288 (2016) 135–143.
[30] H.C. Hamaker, Formation of a deposit by electrophoresis, Trans. Faraday Soc. 35 (1940) 279–287.
[31] V.D. Papachristos, C.N. Panagopoulos, L.W. Christoffersen, A. Markaki, Young's modulus, hardness and scratch adhesion of Ni–P–W multilayered alloy coatings produced by pulse plating, Thin Solid Films 396 (2001) 173–182.
[32] P. Benjamin, C. Weaver, Measurement of adhesion of thin films, Proc. R. Soc. Lond. A Math. Phys. Sci. 254 (1960) 163–176.
[33] P.B. Kadolkar, T.R. Watkins, J.T.M. De Hosson, B.J. Kooi, N.B. Dahotre, State of residual stress in laser-deposited ceramic composite coatings on aluminum alloys, Acta Mater. 55 (2007) 1203–1214.
[34] L. Wang, Y. Gao, H. Liu, Q. Xue, T. Xu, Effects of bivalent co ion on the co-deposition of nickel and nano-diamond particles, Surf. Coat. Technol. 191 (2005) 1–6.
[35] Y. Ootani, J. Xu, T. Hatano, M. Kubo, Contrasting roles of water at sliding interfaces between silicon-based materials: first-principles molecular dynamics sliding simulations, J. Phys. Chem. C 122 (2018) 10459–10467.
[36] T. Han, C. Zhang, X. Chen, J. Li, W. Wang, J. Luo, Contribution of a tribo-induced silica layer to macroscale superlubricity of hydrated ions, J. Phys. Chem. C 123 (2019) 20270–20277.